

## Revisiting the measurement of the spin relaxation time in graphene-based devices

H. Idzuchi,<sup>1,\*</sup> A. Fert,<sup>2</sup> and Y. Otani<sup>1,3,†</sup>

<sup>1</sup>Center for Emergent Matter Science, RIKEN, 2-1 Hirosawa, Wako 351-0198, Japan

<sup>2</sup>Unité Mixte de Physique CNRS/Thales, France associée à l'Université de Paris-Sud, 91405 Orsay, France

<sup>3</sup>Institute for Solid State Physics, University of Tokyo, Kashiwa 277-8581, Japan

(Received 2 November 2014; revised manuscript received 7 May 2015; published 23 June 2015)

A long spin relaxation time ( $\tau_{sf}$ ) is the key for the applications of graphene to spintronics but the experimental values of  $\tau_{sf}$  have been generally much shorter than expected. We show that the usual determination by the Hanle method underestimates  $\tau_{sf}$  if proper account of the spin absorption by contacts is lacking. By revisiting series of experimental results and taking into account the spin absorption, we find that the corrected  $\tau_{sf}$  are longer and, for series of graphene samples of the same fabrication, less dispersed, which leads to a more unified picture of the  $\tau_{sf}$ .

DOI: [10.1103/PhysRevB.91.241407](https://doi.org/10.1103/PhysRevB.91.241407)

PACS number(s): 72.80.Vp, 72.25.Hg, 72.25.Mk

Spin transport in graphene has strongly attracted attention from the perspective of the long spin relaxation time expected from the small spin-orbit coupling of carbon [1–3]. Spin transport to long distances without spin relaxation, with also the additional interest of the low dissipation of spin currents, is promising for the spintronic devices, in particular to merge functionalities of magnetic nonvolatile memory and logic operation, for which a long spin diffusion length  $\lambda_{sf}$  enables multimemory elements to function as sources of spin current for input operation via spin-torque switching [4]. However, the spin relaxation times  $\tau_{sf}$  derived from experiments [5–11], rarely above 1 ns, are much shorter than theoretically expected and also largely dispersed. For example, Volmer *et al.* [10,12] (see Fig. 1(d) in Ref. [10]) have clearly highlighted the broad dispersion of  $\tau_{sf}$  in a wide-ranging series of samples and also pointed out the puzzling general trend of an increase of  $\tau_{sf}$  at increasing resistance of the MgO tunnel junction with the magnetic electrodes.

Spin transport in a nonmagnetic conductor NM (metal, semiconductor, or graphene) is generally studied [13–19] by using lateral spin valves (LSVs) on which two ferromagnetic (FM) wires are bridged by a nonmagnetic (NM) channel. A spin current is injected from one of the magnetic electrodes and one measures a nonlocal spin signal related to the spin accumulation in the NM channel. A frequent method to derive the spin relaxation time is to analyze the variation of the spin signal induced by collective spin precession in an applied field, the so-called Hanle effect [18,19]. An important point is that, without a large enough resistance of the contact between channel and electrodes, a part of the injected spin current is reabsorbed by the electrodes (the so-called back-flow current) if the spin resistance  $R_N = \lambda_{sf}\rho_N/A_N$ , where  $\rho_N$  is the electrical resistivity and  $A_N$  is the cross section of the NM channel (we first suppose a 3D conductor), is larger than the corresponding spin resistance of the FM electrodes [13–15]. Although the possible effect of the spin absorption by contacts has been described analytically and numerically in a couple of publications [9,20,21], most of the determinations of the spin relaxation have been performed by analyzing

Hanle experiments in a standard model [19] that does not take into account the spin absorption by contacts and the resulting correction. How strongly the spin absorption affects the determination of the spin relaxation time in real cases was still controversial and had to be cleaned up. Here we present analytical expressions [20,22] of the effect of spin absorption on Hanle curves, and by taking several examples of prior results by different groups [5,10,12], we show that, except for some of the highest contact resistances (tunnel junction resistances), the spin relaxation time had been significantly underestimated. The correction of this underestimate allows us to reduce the dispersion of the spin relaxation times. We can also indicate the values needed for the contact resistances to avoid important spin absorption effects in large ranges of several parameters such as spin diffusion length, spin resistance, and channel length  $L$ .

First of all, we stress here that the spin absorption is more pronounced in the case of graphene compared to metals. Generally, the spin absorption due to contacts in metallic devices can be easily suppressed with contacts through tunnel junctions. The previous studies by some of us (Idzuchi and Otani) and collaborators clearly showed that, compared to LSVs with metallic contacts, the spin signal  $\Delta R_S$  was strongly enhanced by suppression of spin absorption [23] with  $\text{Ni}_{80}\text{Fe}_{20}(\text{Py})/(\text{MgO})/\text{Ag}$  contacts, as shown in Fig. 1(a), where  $\Delta R_S$  increases more than an order of magnitude with varying  $R_I$  from 0.1 to 10  $\Omega$ . The spin signal  $\Delta R_S$  is reduced by the spin absorption if the contact resistance  $R_I$  is smaller than the spin resistance  $R_N$  of the lateral channel. The different resistance scale of the required contact resistance for metals and graphene comes from the fact that, in typical LSVs with graphene, the channel spin resistance ( $\sim 10$  k $\Omega$ ) is much larger than with metals [ $R_N \sim 0.8$   $\Omega$  for Ag in Fig. 1(a)]. But the fundamental frameworks of spin transport are described in the same manner by replacing the ratio thickness/resistivity of a nonmagnetic metal  $t_N/\rho_N$  by the sheet conductance of graphene  $\sigma_G$  so that the spin resistance of graphene channel is written as  $R_N = \lambda_N/(\sigma_G w_N)$ , where  $\lambda_N$  is the spin diffusion length and  $w_N$  is the channel width. The analytical formulation of the absorption effect on Hanle curves was recently established by two of the authors (Idzuchi and Otani) and collaborators explaining the reason why the spin transport parameters derived from Hanle curves without taking into account the spin absorption differ from the intrinsic

\*idzuchi@riken.jp

†yotani@riken.jp

ones [22]. With spin absorption the Hanle voltage is expressed as

$$\frac{V}{I} = -2R_N \left( \frac{P_{F1}}{1 - P_{F1}^2} \frac{R_{F1}}{R_N} + \frac{P_{I1}}{1 - P_{I1}^2} \frac{R_{I1}}{R_N} \right) \left( \frac{P_{F2}}{1 - P_{F2}^2} \frac{R_{F2}}{R_N} + \frac{P_{I2}}{1 - P_{I2}^2} \frac{R_{I2}}{R_N} \right) \frac{C_{12}}{\det(\hat{X})}, \quad (1)$$

where  $R_{Ik} = 1/G_{Ik}$  ( $G_{Ik} = G_{Ik}^{\uparrow} + G_{Ik}^{\downarrow}$ ) and  $P_{Ik} = (G_{Ik}^{\uparrow} - G_{Ik}^{\downarrow})/(G_{Ik}^{\uparrow} + G_{Ik}^{\downarrow})$  are the interface resistance (conductance) and the conductance spin asymmetry of  $k$ th contact.  $R_{Fk} = (\rho_F \lambda_F / A_{Ik})$  and  $A_{Fk}$  are the spin resistance and cross-sectional area of the FM electrode on  $k$ th contact. The expression  $\det(\hat{X})$  is the determinant of the matrix  $\hat{X}$  and  $C_{12}$  is the (1, 2) component of the cofactors of  $\hat{X}$ , where  $C_{12}$  and  $\hat{X}$  are given by

$$C_{12} = -\det \begin{pmatrix} \text{Re}[\bar{\lambda}_{\omega} e^{-L/\bar{\lambda}_{\omega}}] & -\text{Im}[\bar{\lambda}_{\omega} e^{-L/\bar{\lambda}_{\omega}}] & -\text{Im}[\bar{\lambda}_{\omega}] \\ \text{Im}[\bar{\lambda}_{\omega}] & r_{1\perp} + \text{Re}[\bar{\lambda}_{\omega}] & \text{Re}[\bar{\lambda}_{\omega} e^{-L/\bar{\lambda}_{\omega}}] \\ \text{Im}[\bar{\lambda}_{\omega} e^{-L/\bar{\lambda}_{\omega}}] & \text{Re}[\bar{\lambda}_{\omega} e^{-L/\bar{\lambda}_{\omega}}] & r_{2\perp} + \text{Re}[\bar{\lambda}_{\omega}] \end{pmatrix}, \quad (2)$$

$$\hat{X} = \begin{pmatrix} r_{1\parallel} + \text{Re}[\bar{\lambda}_{\omega}] & \text{Re}[\bar{\lambda}_{\omega} e^{-L/\bar{\lambda}_{\omega}}] & -\text{Im}[\bar{\lambda}_{\omega}] & -\text{Im}[\bar{\lambda}_{\omega} e^{-L/\bar{\lambda}_{\omega}}] \\ \text{Re}[\bar{\lambda}_{\omega} e^{-L/\bar{\lambda}_{\omega}}] & r_{2\parallel} + \text{Re}[\bar{\lambda}_{\omega}] & -\text{Im}[\bar{\lambda}_{\omega} e^{-L/\bar{\lambda}_{\omega}}] & -\text{Im}[\bar{\lambda}_{\omega}] \\ \text{Im}[\bar{\lambda}_{\omega}] & \text{Im}[\bar{\lambda}_{\omega} e^{-L/\bar{\lambda}_{\omega}}] & r_{1\perp} + \text{Re}[\bar{\lambda}_{\omega}] & \text{Re}[\bar{\lambda}_{\omega} e^{-L/\bar{\lambda}_{\omega}}] \\ \text{Im}[\bar{\lambda}_{\omega} e^{-L/\bar{\lambda}_{\omega}}] & \text{Im}[\bar{\lambda}_{\omega}] & \text{Re}[\bar{\lambda}_{\omega} e^{-L/\bar{\lambda}_{\omega}}] & r_{2\perp} + \text{Re}[\bar{\lambda}_{\omega}] \end{pmatrix}, \quad (3)$$

with  $\bar{\lambda}_{\omega} = \tilde{\lambda}_{\omega}/\lambda_N$  and  $\tilde{\lambda}_{\omega} = \lambda_N/\sqrt{1 + i\omega_L \tau_{sf}}$ ,

$$r_{k\parallel} = \left( \frac{2}{1 - P_{Ik}^2} \frac{R_{Ik}}{R_N} + \frac{2}{1 - P_{Fk}^2} \frac{R_{Fk}}{R_N} \right) \quad \text{and} \quad r_{k\perp} = \frac{1}{R_N G_{Ik}^{\uparrow\downarrow}} \quad (k = 1, 2). \quad (4)$$

In the above equation,  $G_{Ik}^{\uparrow\downarrow}$  is the spin mixing conductance. In order to reduce the number of fitting parameters, we assume an isotropic spin absorption without additional absorption of the transverse spin components due to spin transfer. Hence the spin mixing conductance is given by  $G_{Ik}^{\uparrow\downarrow} = 1/(2R_{Ik} + 2R_{Fk})$ . As in the application to LSVs with graphene and Co electrodes ( $\lambda_{Co} = 38$  nm,  $\rho_F = 25$   $\mu\Omega$  cm,  $P_F = 0.36$  [25]), the contact  $R_I$  is at least three orders of magnitude larger than  $R_F$ , so that  $G_{Ik}^{\uparrow\downarrow}$  is practically equal to  $1/(2R_{Ik})$ . In the limit of small spin absorption, Eqs. (1)–(4) reduce to the formula used in the interpretation that does not take into account the spin absorption [22]. We note that the present model does not explicitly include the effect of fringe field and interfacial spin loss. The inset of Fig. 1(a) for the case of metallic LSVs shows that the contact resistance affects not only the amplitude of spin signal but also the width of the Hanle curves. Actually, Eqs. (1)–(4) enables us to explain the different width of Hanle curves in the inset with almost the same spin relaxation time of  $40.3 \pm 5.3$  ps for Py/Ag contacts and  $38.0 \pm 3.9$  ps for Py/MgO/Ag junctions [22].

As shown in Figs. 1(c)–1(e), we have reanalyzed the Hanle curves of Ref. [5] for graphene-based LSVs with contact resistances ranging between the 0.285 and 30 k $\Omega$  sample. All the data are taken at room temperature for graphene of typical conductivity around 0.4 mS and in samples with usual values of  $w_N$  and  $L$  (length) in the micrometer range. For the sample of Fig. 1(c) ( $R_I = 0.285$  k $\Omega$ ), a good fit of the curve is obtained by using the parameters of the first line in Table I, i.e., with the experimental parameters of Ref. [5], and, for the three free parameters,  $\tau_{sf} = 498$  ps,  $P_I = 0.0108$ ,  $D_N = 0.0149$  m<sup>2</sup>/s. It should be noted here that  $\tau_{sf}$  is considerably increased with respect to the value derived without considering the spin absorption,  $\tau_{sf}^* = 84$  ps. In contrast,  $D_N$  decreases from the fitted value without taking account of spin absorption effect

(0.025 m<sup>2</sup>/s) [6,9]. Therefore, in order to characterize intrinsic spin transport properties, it is indispensable to consider the spin absorption which significantly modifies the spatial distribution of the chemical potential inside the nonmagnetic channel [22].

For the sample of Fig. 1(d) with  $R_I = 6$  k $\Omega$  (characterized by Han *et al.* as a sample with pinhole in the tunnel junctions) the spin relaxation time we obtained with the parameters of Table I is 359 ps, whereas  $\tau_{sf}^* = 134$  ps had been obtained without spin absorption [5]. For the sample with a mean value of the tunnel contact resistance respectively equal to 30 and 50 k $\Omega$  in Ref. [5], our analysis of the Hanle curve [see Fig. 1(e) for one of the samples], leads respectively to  $\tau_{sf} = 481$  ps and  $\tau_{sf} = 511$  ps, whereas the standard analysis [4] had led to  $\tau_{sf}^* = 448$  and 495 ps.

All the data are summarized in Fig. 2 by the plot of  $\tau_{sf}$  and  $\tau_{sf}^*$  as a function of the interface resistance for all the samples in Ref. [5]. Whereas the original analysis leads to an apparent continuous contact-induced increase of  $\tau_{sf}^*$  from 84 ps for  $R_I = 0.285$  k $\Omega$  to 495 ps for  $R_I = 50$  k $\Omega$ , we find that, with contact absorption, all the Hanle curves can be accounted for with an almost constant “intrinsic”  $\tau_{sf}$  of about 500 ps and an almost constant  $\lambda_{sf}$  close to 3  $\mu$ m. The increase of spin relaxation time when the spin absorption is taken into account is still by a factor of 2.7 for the sample with relatively close values of  $R_I$  and  $R_N$  (6 and 9.11 k $\Omega$ , respectively). The correction factor still amounts to 7% (3%) for the interface resistance as large as 30 k $\Omega$  (50 k $\Omega$ ). In our model, a precise determination of  $\tau_{sf}$  can be affected by the uncertainty of the other parameters, but these variations are small compared to the total correction. (See Supplemental Material [26]. Also we note that Ref. [5] pointed out the existence of contact-induced spin relaxation but did not report any quantitative analysis.)

An apparent increase of spin relaxation time with the contact resistance similar to that in Ref. [5] was also reported

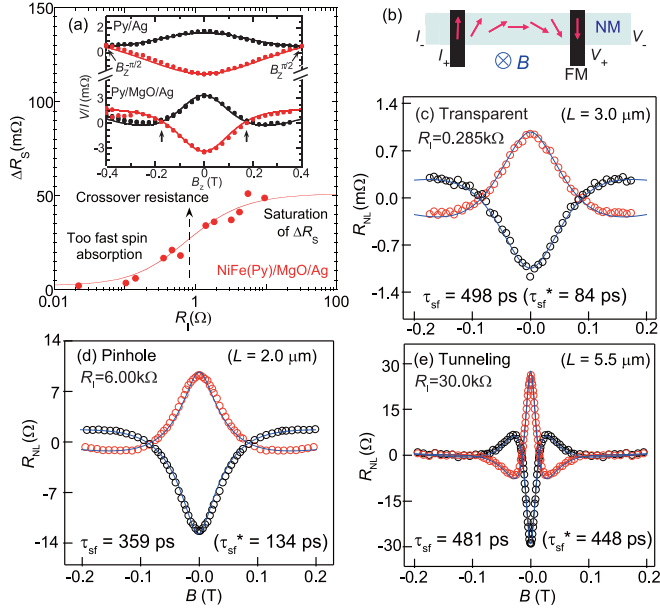


FIG. 1. (Color online) (a) Nonlocal spin signal  $\Delta R_S$  as a function of contact resistance  $R_I$  for NiFe/Ag/NiFe lateral spin valves (LSVs) with MgO layer between NiFe(Py) and Ag, for the separation  $L = 0.30$   $\mu$ m [23]. The crossover resistance between the conductivity mismatch regime (too fast spin absorption by the contacts) and saturation (intrinsic spin relaxation in Ag)  $R_{\text{crossover}} = R_N = \rho_{\text{Ag}} \lambda_{\text{Ag}} / t_{\text{Ag}} w_{\text{Ag}}$  is the scale governing the variation with  $R_I$  [24] and is of the order of 1  $\Omega$  for a metal as Ag [resistivity  $\rho_{\text{Ag}}$  in the  $\mu\Omega$  cm range, spin diffusion length  $\lambda_{\text{Ag}}$  around 1  $\mu$ m, and the thickness  $t_{\text{Ag}}$  (width  $w_{\text{Ag}}$ ) in the 10<sup>1</sup> nm (10<sup>2</sup> nm) range]. Inset: Example of the different widths of Hanle curves for two LSVs with different contact resistances. Taking into account the spin absorption enables a fit of the Hanle curves of the two samples (see solid lines) with practically the same spin relaxation time. (b) Schematic illustration of Hanle measurement. Larmor precession of spin current is observed electrically. (c) Reanalysis of Hanle curves for single layer graphene lateral spin valves with transparent contacts ( $R_I = 0.285$  k $\Omega$ ), (d) with pinhole in the tunnel contacts ( $R_I = 6$  k $\Omega$ ), and (e) with tunnel junctions ( $R_I = 30$  k $\Omega$ ).  $\tau_{sf}$  is the intrinsic spin relaxation time derived from the model with the effect of spin absorption, whereas the spin relaxation time  $\tau_{sf}^*$  is derived without taking into account the spin absorption (standard model) in Ref. [5].

by the Aachen group [10,12] and we have found that its main features can also be explained by the effect of spin absorption. As shown in the Supplemental Material [26] for one of the sample series, we could also interpret the apparent

TABLE I. Parameters for the interpretation of Hanle signals in Figs. 1(c)–1(e).  $R_I$ ,  $\sigma_G$ ,  $L$ ,  $w_N$  are from Ref. [5],  $D_N$ ,  $P_I$ , and  $\tau_{sf}$  are the free parameters ( $\lambda_N$  and  $R_N$  are the corresponding values of the spin diffusion length and spin resistance), and  $\tau_{sf}^*$  is the spin relaxation in the previous interpretation [5] in a model without spin absorption.  $P_I$  shown with † was the geometric mean of  $P_I$  for Hanle curves with parallel and antiparallel magnetic configurations.

Junction	$R_I$ (k $\Omega$ )	$\sigma_G$ (mS)	$L$ ( $\mu$ m)	$w_N$ ( $\mu$ m)	$D_N$ (m <sup>2</sup> /s)	$P_I$	$\tau_{sf}$ (ps)	$\lambda_N$ ( $\mu$ m)	$R_N$ (k $\Omega$ )	$\tau_{sf}^*$ (ps)
Transparent	0.285	0.44	3.00	1.00	0.0149	0.0108	498	2.72	6.18	84
Pinhole	6.00	0.27	2.00	1.00	0.0168	0.120†	359	2.46	9.11	134
Tunnel	30.0	0.29	5.50	2.20	0.0134	0.0810	481	2.54	4.26	448
Tunnel	50.0	0.29	2.10	2.20	0.0176	0.156†	511	3.00	4.70	495

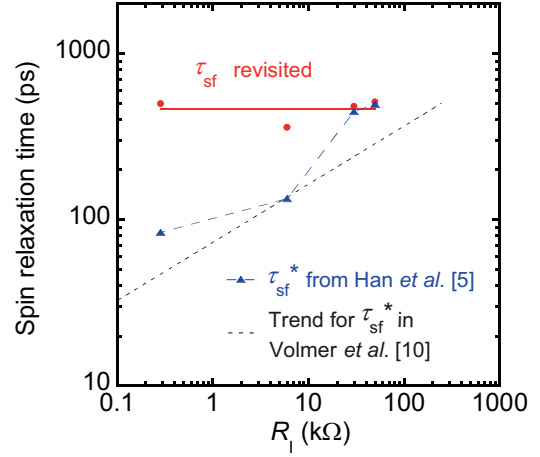


FIG. 2. (Color online) Comparison of the spin relaxation time  $\tau_{sf}$  (circles) and  $\tau_{sf}^*$  (triangles), respectively, derived from experimental Hanle curves [5] in models with (this paper) and without (Han et al. [5]) spin absorption by contacts for samples of various contact resistances  $R_I$ . The thick dashed line connecting the triangles is a guide to the eyes. The thin dashed line is the approximate trend of the similar increase of the noncorrected  $\tau_{sf}^*$  at increasing contact resistance for a series of samples in Ref. [10]. We show in the Supplemental Material [26] that, when the contact absorption is taken into account (our model), all the data in Ref. [10] can be approximately fitted with a unique value of  $\tau_{sf}$ .

increase of the spin relaxation time with the contact resistance by taking into account the effect of spin absorption on the Hanle curves and accounting for all the data with a single and longer value of  $\tau_{sf}$ . One of the authors of the Aachen publications [27] commented that the correction due to spin absorption can reduce the gap between determinations by Hanle measurements and other methods.

Finally, after having illustrated the influence of the spin absorption by the contacts in the specific case of the sample in Refs. [5,10], we will describe how, more generally, the effect of the contacts varies in different parameter ranges. In Fig. 3(a) we show the correction factor  $\tau_{sf}/\tau_{sf}^*$  as a function of  $R_I/R_N$  for several values of the ratio  $L/\lambda_N$  (the other parameters are typical for graphene:  $\sigma_G = 0.335$  mS,  $P_I = 0.1$ ,  $w_N = 1.0$   $\mu$ m,  $D_N = 0.010$  m<sup>2</sup>/s). The Hanle curves are first calculated using our model with spin absorption for a series of values for  $\tau_{sf}$  (which give the corresponding values of  $\lambda_N$  and  $R_N$ ). Then, in a second stage, the “noncorrected relaxation time”  $\tau_{sf}^*$  is derived from fitting these curves to the standard

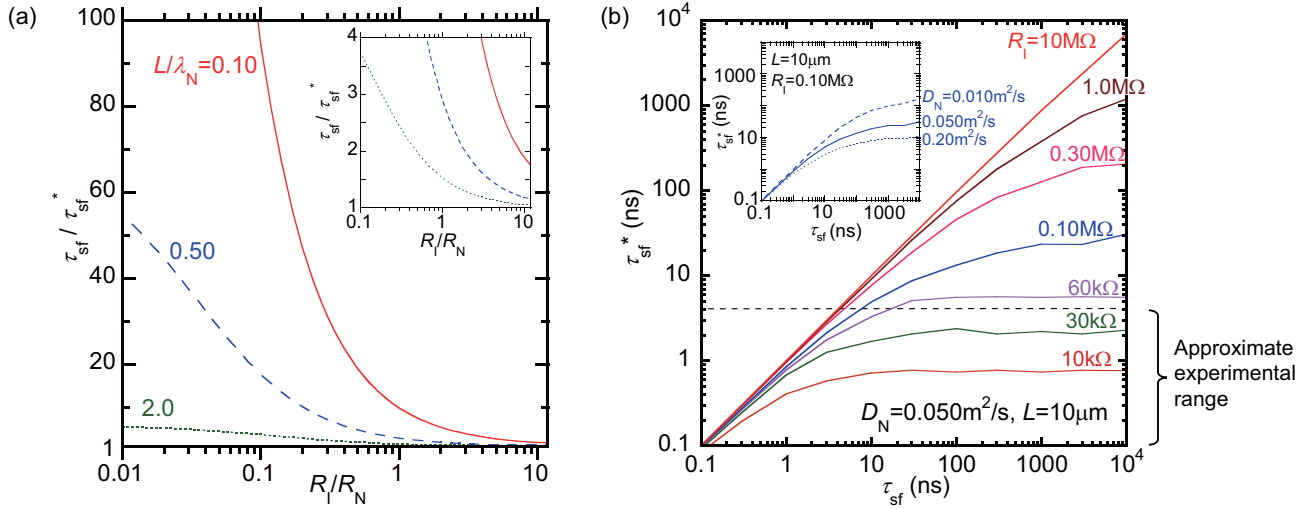


FIG. 3. (Color online) (a) General variation of the spin absorption correction factor of the spin relaxation time  $\tau_{sf}/\tau_{sf}^*$  as a function of  $R_1/R_N$  for several values of  $L/\lambda_N$ . The correction factor is large for  $R_1/R_N < 1$  (strong spin absorption) but it can also be significant for values of  $R_1$  as large as 5–10  $R_N$  if the channel length is shorter than the spin diffusion length. Curves were calculated with typical parameter for graphene:  $\sigma_G = 0.335$  mS,  $P_1 = 0.1$ ,  $w_N = 1.0$   $\mu$ m,  $D_N = 0.010$  m<sup>2</sup>/s. (b) Uncorrected  $\tau_{sf}^*$  vs intrinsic  $\tau_{sf}$  for several values of  $R_1$  calculated for graphene LSVs with, in addition to the parameters used in (a),  $L = 10$   $\mu$ m and a typical value for  $D_N = 0.050$  m<sup>2</sup>/s for recent high mobility graphene device [28]. One sees that even a contact resistance of 100 k $\Omega$  is not enough large to block spin absorption. Typical value for  $\lambda_N$  is given by  $\lambda_N = (D_N \tau_{sf})^{1/2} = 10$   $\mu$ m for  $D_N = 0.05$  m<sup>2</sup>/s and  $\tau_{sf} = 2$  ns. Inset shows influence of values of  $D_N$  for  $R = 100$  k $\Omega$ , where dashed (dotted) line is for value of  $D_N = 0.010$  m<sup>2</sup>/s (0.20 m<sup>2</sup>/s) on both sides of solid curve for  $D_N = 0.050$  m<sup>2</sup>/s.

expression without spin absorption [19]. It turns out that the correction factor becomes very large when  $L$  is shorter than  $\lambda_N$ . With  $L/\lambda_N = 0.1$ ,  $\tau_{sf}/\tau_{sf}^*$  is about 10 for  $R_1 = R_N$  and is still 1.6 for  $R_1 = 10R_N$ . This means that, for example with a sample of graphene of sheet resistivity 1 k $\Omega$  and  $\lambda_N = 10$   $\mu$ m, and a LSV with  $L = 1$   $\mu$ m and  $w_N = 1$   $\mu$ m (resulting in  $R_N = 10$  k $\Omega$ ), the correction factor is still as large as 1.6 for  $R_1 = 10R_N = 100$  k $\Omega$ , the resistance larger than that of most tunnel resistance used up to now in graphene LSVs.

In Fig. 3(b) the solid lines indicate how, for different values of  $R_1$  and with the same value of  $\sigma_G$ ,  $P_1$ ,  $w_N$  as in Fig. 3(a),  $L = 10$   $\mu$ m and  $D_N = 0.05$  m<sup>2</sup>/s, which is a typical value found with high mobility graphene in recent experiments [28], the  $\tau_{sf}^*$  derived from a noncorrected interpretation of Hanle curves [19] varies as a function of the  $\tau_{sf}$  used to calculate these curves. It turns out that, when the intrinsic spin relaxation time  $\tau_{sf}$  is long, the noncorrected  $\tau_{sf}^*$  is more strongly underestimated, much more than in our above re-interpretation of the situation with relaxation times below 1 ns in Ref. [5]. More precisely we find that, even for large values of  $R_1$ , the noncorrected  $\tau_{sf}^*$  does not follow the increase of  $\tau_{sf}$  above a threshold value of  $\tau_{sf}$  and levels off at a saturation value. Taking  $R_1 = 60$  k $\Omega$  as a typical example, we find that the Hanle curves no longer change and the noncorrected  $\tau_{sf}^*$  levels off at about 7 ns for  $\tau_{sf}$  increasing largely above 10 ns. In other words, even with such a large value of interface resistance, an increase of  $\tau_{sf}$  above the 10 ns range cannot be detected if the absorption by contacts is not taken into account, the standard analysis giving only a lower bound of  $\tau_{sf}$ . For a  $\tau_{sf}$  of 50 ns and the parameters of the simulation, one sees in Fig. 3(b) that a resistance as large as 300 k $\Omega$  is needed to obtain a reasonable estimate of

the relaxation time in a standard analysis. Larger  $D_N$  gives more pronounced effect as shown in the inset of Fig. 3(b) because of larger spin absorption effect. We can suggest that values of  $\tau_{sf}$  above the 10 ns range could have been found in recent experiments if account of the contact absorption had been taken in the numerical analysis of the Hanle measurements.

In summary, we have revisited Hanle curves of graphene LSVs which were previously analyzed [5] by using the “standard” model without spin absorption [10,18]. Our reanalysis shows that the reported difference in the spin relaxation times of samples with different contact resistances is due to the interface effects. After correction of these effects the spin relaxation times are much less dispersed. A similar reanalysis of other experimental data [10] is presented in the Supplemental Material [26]. A general discussion based on the results of Fig. 3 shows that, without correction for the back flow and the spin absorption through contacts, and even with contact resistances in the 100 k $\Omega$  range for usual device geometries the spin relaxation time is significantly underestimated when its intrinsic value is above the nanosecond range. We hope that our discussion on the underestimate of the spin relaxation time in analyses of standard Hanle analyses can be useful to understand the differences with data derived from another approach [8]. A more general conclusion is that one can be more optimistic about spin relaxation in graphene and its potential for spintronics.

We acknowledge a helpful discussion with B. Beschoten. This work was partly supported by Grant-in-Aid for Scientific Research on Innovative Area, “Nano Spin Conversion Science” (Grant No. 26103002).

- [1] N. Tombros, C. Jozsa, M. Popinciuc, H. T. Jonkman, and B. J. van Wees, *Nature (London)* **448**, 571 (2007).
- [2] D. Pesin and A. H. MacDonald, *Nat. Mater.* **11**, 409 (2012).
- [3] W. Han, R. K. Kawakami, M. Gmitra, and J. Fabian, *Nat. Nanotech.* **9**, 794 (2014).
- [4] B. Behin-Aein, D. Datta, S. Salahuddin, and S. Datta, *Nat. Nanotech.* **5**, 266 (2010).
- [5] W. Han, K. Pi, K. M. McCreary, Y. Li, J. J. I. Wong, A. G. Swartz, and R. K. Kawakami, *Phys. Rev. Lett.* **105**, 167202 (2010).
- [6] W. Han and R. K. Kawakami, *Phys. Rev. Lett.* **107**, 047207 (2011).
- [7] T. Y. Yang, J. Balakrishnan, F. Volmer, A. Avsar, M. Jaiswal, J. Sann, S. R. Ali, A. Pachoud, M. Zeng, M. Popinciuc, G. Güntherodt, B. Beschoten, and B. Özyilmaz, *Phys. Rev. Lett.* **107**, 047206 (2011).
- [8] B. Dlubak, M.-B. Martin, C. Deranlot, B. Servet, S. Xavier, R. Mattana, M. Sprinkle, C. Berger, W. A. De Heer, F. Petroff, A. Anane, P. Seneor, and A. Fert, *Nat. Phys.* **8**, 557 (2012).
- [9] T. Maassen, I. J. Vera-Marun, M. H. D. Guimarães, and B. J. van Wees, *Phys. Rev. B* **86**, 235408 (2012).
- [10] F. Volmer, M. Drögeler, E. Maynicke, N. von den Driesch, M. L. Boschen, G. Güntherodt, and B. Beschoten, *Phys. Rev. B* **88**, 161405 (2013).
- [11] M. Wojtaszek, I. J. Vera-Marun, T. Maassen, and B. J. van Wees, *Phys. Rev. B* **87**, 081402(R) (2013).
- [12] G. Schmidt, D. Ferrand, L. W. Molenkamp, A. T. Filip, and B. J. van Wees, *Phys. Rev. B* **62**, R4790(R) (2000).
- [13] F. Volmer, M. Drögeler, E. Maynicke, N. von den Driesch, M. L. Boschen, G. Güntherodt, C. Stampfer, and B. Beschoten, *Phys. Rev. B* **90**, 165403 (2014).
- [14] E. I. Rashba, *Phys. Rev. B* **62**, R16267 (2000).
- [15] A. Fert and H. Jaffrès, *Phys. Rev. B* **64**, 184420 (2001).
- [16] S. Maekawa, *Concepts in Spin Electronics* (Oxford University Press, New York, 2006).
- [17] A. Brataas, G. Bauer, and P. Kelly, *Phys. Rep.* **427**, 157 (2006).
- [18] M. Johnson and R. H. Silsbee, *Phys. Rev. Lett.* **55**, 1790 (1985).
- [19] F. Jedema, H. Heersche, A. T. Filip, J. Baselmans, and B. J. van Wees, *Nature (London)* **416**, 713 (2002).
- [20] M. Popinciuc, C. Józsa, P. J. Zomer, N. Tombros, A. Veligura, H. T. Jonkman, and B. J. van Wees, *Phys. Rev. B* **80**, 214427 (2009).
- [21] E. Sosenko, H. Wei, and V. Aji, *Phys. Rev. B* **89**, 245436 (2014).
- [22] H. Idzuchi, Y. Fukuma, S. Takahashi, S. Maekawa, and Y. Otani, *Phys. Rev. B* **89**, 081308 (2014).
- [23] Y. Fukuma, L. Wang, H. Idzuchi, S. Takahashi, S. Maekawa, and Y. Otani, *Nat. Mater.* **10**, 527 (2011).
- [24] S. Takahashi and S. Maekawa, *Phys. Rev. B* **67**, 052409 (2003).
- [25] L. Piraux, S. Dubois, A. Fert, and L. Belliard, *Eur. Phys. J. B* **4**, 413 (1998).
- [26] See Supplemental Material at <http://link.aps.org/supplemental/10.1103/PhysRevB.91.241407> for detail analysis and reanalysis of other experimental data [10].
- [27] B. Beschoten (private communication).
- [28] M. H. D. Guimarães, P. J. Zomer, J. Ingla-Aynés, J. C. Brant, N. Tombros, and B. J. van Wees, *Phys. Rev. Lett.* **113**, 086602 (2014).